Validation of a histamine H$_3$ receptor model through structure–activity relationships for classical H$_3$ antagonists

Simone Lorenzi,[a] Marco Mor,[a,*] Fabrizio Bordi,[a] Silvia Rivara,[a]
Mirko Rivara,[a] Giovanni Morini,[a] Simona Bertoni,[b]
Vigilio Ballabeni,[b] Elisabetta Barocelli[b] and Pier Vincenzo Plazzi[a]

[a]*Dipartimento Farmaceutico, Università degli Studi di Parma, Parco Area delle Scienze 27/A, I-43100 Parma, Italy*
[b]*Dipartimento di Scienze Farmacologiche, Biologiche e Chimiche Applicate, Università degli Studi di Parma,
Parco Area delle Scienze 27/A, I-43100 Parma, Italy*

Abstract—Histamine H$_3$ receptor is a G protein-coupled receptor whose activation inhibits the synthesis and release of histamine and other neurotransmitters from nerve endings and is involved in the modulation of different central nervous system functions. H$_3$ antagonists have been proposed for their potential usefulness in diseases characterized by impaired neurotransmission and they have demonstrated beneficial effects on learning and food intake in animal models. In the present work, a 3D model of the rat histamine H$_3$ receptor, built by comparative modeling from the crystallographic coordinates of bovine rhodopsin, is presented with the discussion of its ability to predict the potency of known and new H$_3$ antagonists. A putative binding site for classical, imidazole-derived H$_3$ antagonists was identified by molecular docking. Comparison with a known pharmacophore model and the binding affinity of a new rigid H$_3$ antagonist (compound **1**, pK_i = 8.02) allowed the characterization of a binding scheme which could also account for the different affinities observed in a recently reported series of potent H$_3$ antagonists, characterized by a 2-aminobenzimidazole moiety. Molecular dynamics simulations were employed to assess the stability and reliability of the proposed binding mode. Two new conformationally constrained benzimidazole derivatives were prepared and their binding affinity was tested on rat brain membranes; compound **9**, designed to reproduce the conformation of a known potent H$_3$ antagonist, showed higher potency than compound **8**, as expected from the binding scheme hypothesized.
© 2005 Elsevier Ltd. All rights reserved.

1. Introduction

The superfamily of G protein-coupled receptors (GPCRs) includes a large number of membrane-associated proteins, involved in the regulation of a variety of physiological processes. The abundance of these receptors, their ubiquitous distribution, their involvement in different diseases, and the large number of endogenous substances and drugs interacting with them have led to the study of these proteins as traditional targets for medicinal chemistry research. Recently, the use of three-dimensional (3D) models of GPCRs, built by comparative modeling from the rhodopsin crystallographic structure, proved to be useful for drug design and structure–activity relationship (SAR) investigations. Among the endogenous substances exerting their effects through GPCRs, histamine interacts with four types of receptors, which differ in distribution, pharmacology, and function. The H$_1$ receptor[1] is a post-synaptic one, principally involved in allergic reactions; the H$_2$ receptor has post-synaptic localization and is primarily involved in the regulation of gastric secretion; the H$_4$ one is mainly located in cells of immunological relevance, such as T cells, neutrophils, and monocytes.[2,3] The third receptor subtype (H$_3$) was identified by Arrang et al. in 1983,[4] and it is expressed with the highest abundance in the central nervous system. The H$_3$ receptor has generally pre-synaptic localization and inhibits the synthesis and release of histamine[5] and other neurotransmitters, like acetylcholine,[6] serotonin,[7] noradrenaline,[8] and dopamine.[9] Its involvement in different brain functions, like learning processes and regulation of food intake, has led to the proposal of H$_3$ antagonists for different therapeutic applications,[10,11] especially in the treatment of

Alzheimer's disease,[12] attention deficit hyperactivity disorder (ADHD),[13] epilepsy,[14] and obesity.[15]

The first H_3 antagonists maintained the imidazole ring of the natural agonist, histamine, and were characterized by the presence of a polar fragment, connected to the imidazole through an alkyl spacer, and by the presence of an ending lipophilic group.[16] The central polar fragment can be very different, including guanidine, amide, amine, ether, carbamate, thiourea, or isothiourea groups,[17] or heterocyclic rings, like pyridine,[18] oxadiazole,[19] imidazole,[20,21] thiazole,[22] and their benzocondensed analogs,[23,24] but it can also be replaced by non-polar groups, like in the alkyne derivative cipralisant (GT-2331).[25] The polar fragment can be neutral at physiological pH, as in the reference antagonist thioperamide,[26] or mainly protonated, as the isothioureic fragment of the potent antagonist clobenpropit[27] (Fig. 1). Compounds having the above-mentioned structural features will be referred to as 'classical' H_3 antagonists, to differentiate them from H_3 antagonists lacking the imidazole ring, which have been recently described.[28–33]

Several structure–activity relationship studies based on molecular models of classical H_3 antagonists have been reported, leading to pharmacophore[34] or 3D-QSAR[35] models. In particular, recent investigations by De Esch et al. pointed out that thioperamide and clobenpropit could be mutually superposed following a common pharmacophore model,[36] and that the cyclohexyl substituent of thioperamide could be replaced by the benzyl one found in clobenpropit with only a moderate reduction of receptor affinity.[37] The proposed pharmacophore model suggested the existence of two lipophilic pockets in the H_3 receptor antagonist binding site, and the possibility that both a neutral and a strongly basic polar fragment could be accommodated with similar arrangements at the same binding site.[34]

A series of potent classical H_3 antagonists, 2-(imidazolyl-alkyl-amino)-benzimidazole derivatives recently described by our group,[38] includes compounds with subnanomolar binding affinity at rat brain H_3 receptors. This series is characterized by a polar fragment inscribed into a 2-aminobenzimidazole nucleus, also containing a lipophilic portion, which has moderate basicity (pK_a around 6.5) and can therefore be regarded as a bridge structure between neutral and strongly basic polar groups. SAR investigations on this series led us to modify the spacer length (two or three methylenes) and to explore the effect of N-methylation at the 2-aminobenzimidazole group.[39] We observed that compounds with the shorter spacer were less potent and that the SAR profiles for N-methyl derivatives were opposite in the two cases (Table 1). These results were hardly explained by pharmacophore analysis, and they needed a topographical model of rat H_3 receptor to be rationalized.
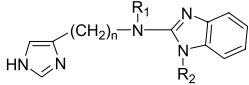
The superfamily of GPCRs can be divided into five major classes; within each class the sequence homology among different proteins is generally low, but considerable similarity in their tertiary structure is presumed from topological properties (i.e., hydrophobic and hydrophilic domains) and from conserved structural and functional domains, like disulfide bonds or the E/DRY motif.[40,41] Bovine rhodopsin (BR) is the major representative of class A GPCRs, which also includes receptors for the biogenic amines like dopamine, serotonin, noradrenaline, and histamine, and it is the only one whose crystallographic coordinates are available.[42] The building of a reliable receptor model by homology modeling requires high sequence similarity.[40] However, although in the case of GPCRs the similarity is generally low, the alignment can be based on key features, like hydrophobicity patterns, structural (disulfide bonds) and functional (aromatic clusters, E/DRY motif, NPXXY motif) microdomains. In fact, BR had been generally employed as a template for homology modeling of receptors belonging to this class,[43,44] even if attention should be paid to model validation, assessing its ability to explain known SAR.[45]

Many studies have contributed to characterize the binding site of histamine within the H_3 receptor, where two acidic amino acids proved to be necessary for agonist binding. One of these is D114 (Asp114, or D3.32, according to the numbering rules proposed by
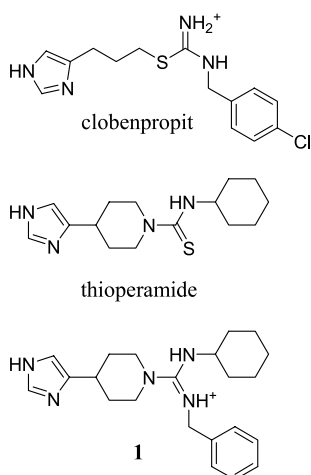
Figure 1. Classical H_3 receptor antagonists and the newly synthesized compound **1** employed for binding site identification, represented in the protonation state applied for molecular modeling calculations.

Table 1. Binding affinity at rat H_3 receptors of 2-aminobenzimidazole derivatives

Compound	R_1	R_2	n	pK_i^a
2	H	H	2	7.25
3	CH_3	H	2	6.26
4	H	CH_3	2	7.71
5	H	H	3	8.90
6	CH_3	H	3	8.60
7	H	CH_3	3	6.83

[a] From Refs. [38] and [39].

Ballesteros et al.),[40] highly conserved through class A of GPCRs[46,47] and among all aminergic receptors,[48] which is presumed to bind the charged amino group of the natural ligand.[49,50] Mutation of the corresponding D3.32 in the H_1 receptor revealed that this amino acid is essential for both agonist and antagonist binding.[51] Mutagenesis studies of the amino acids in TM5 of the H_3 receptor have highlighted that a mutation of E206 (Glu206 or E5.46) to Ala decreased the affinity of histamine and of the subtype selective agonist R-α-methylhistamine by more than 2000 times.[49] This amino acid is thought to interact with the imidazole ring of histamine, on the basis of mutagenesis data of the corresponding amino acids in the H_1[52,53] and H_2 receptors.[50] Moreover, this amino acid corresponds to Ser207 of the β2 receptor, which was found to interact with the catechol ring of adrenaline.[54] Mutagenesis data on the H_4 receptor, which has the highest sequence similarity with the H_3 subtype, are in accordance with the essential role of D3.32 and E5.46 for histamine binding.[55] Given the presence of the imidazole ring in H_3 agonists, like histamine, and in the classical H_3 antagonists, it is reasonable to suppose that the binding site of the two kinds of ligands is common, at least in part.

Sequence alignment and docking of ligands within a 3D receptor model strongly influence the definition of the putative binding site and of the binding scheme for ligands. A validation of the model, based on SAR considerations and on the design and synthesis of new ligands, is therefore necessary to afford its usefulness in drug design. Three models of the H_3 receptor have been recently reported, leading to corresponding hypotheses of interaction with two classes of antagonists. The first model, proposed by Stark et al.,[56] analyzed the binding mode of proxyfan (3-benzyloxypropyl-imidazole) and its derivatives, having a phenol ether as the so-called polar fragment; their imidazole ring is hydrogen-bonded to E206 in TM5, whereas no interaction is reported for the oxygen atom. The second model, described by Yao et al.,[57] proposed a different binding mode for H_3 ligands, both agonists and antagonists, with no interaction between histamine imidazole and E206. The third model reported the binding mode of histamine only, which interacted with both E206 and D114.[49] Although describing interesting aspects of the binding site shape, these models did not deeply investigate the role of the central polar fragment of classical H_3 antagonists in receptor binding.

In this work, we built a 3D model of rat H_3 receptor and we developed a binding scheme for classical H_3 antagonists, starting from the hypothesis that their imidazole ring interacts with E206, pointing our attention to the role of the central polar fragment found in basic (i.e., clobenpropit) and neutral (i.e., thioperamide) ligands, looking for a common interaction model. The model thus obtained was employed to rationalize the SARs previously observed for the aforementioned series of 2-aminobenzimidazole derivatives. Moreover, new compounds, endowed with limited conformational flexibility, were synthesized and tested on rat brain membranes to validate some structural requirements of the putative binding site.

2. Chemistry

Newly synthesized compounds, **1**, **8**, and **9** were prepared following different synthetic routes. According to Scheme 1, N-benzyl-N'-cyclohexyl-4-(1H-imidazol-4-yl)-piperidine-1-carboxamidine (**1**) was synthesized by reaction of 4-(1H-imidazol-4-yl)-piperidine (**10**) with benzyl-cyclohexyl-carbodiimide (**11**). 4-(1H-Imidazol-4-yl)-piperidine was synthesized as described by Windhorst et al.[58] and benzyl-cyclohexyl-carbodiimide was prepared following the procedures by Jaszay et al.[59] and Liu et al.[60] The two 2-aminobenzimidazole derivatives with reduced conformational freedom, 2-[4-(1H-imidazol-4-yl)-piperidin-1-yl]-1H-benzimidazole (**8**) and 2-[3-(1H-imidazol-4-ylmethyl)-piperidin-1-yl]-1H-benzimidazole (**9**), were synthesized by the condensation of 2-chlorobenzimidazole with **10** and 3-(1H-imidazol-4-ylmethyl)-piperidine (**12**), respectively, as represented in Scheme 2. The last intermediate, 3-(1H-imidazol-4-ylmethyl)-piperidine, was prepared following the synthetic route proposed by Vollinga et al.[61]

3. Pharmacology

H_3 receptor affinity of the newly synthesized compounds was measured by displacement of [³H]-(R)-α-methylhistamine ([³H]RAMHA) bound to rat cerebral cortex synaptosomes. The antagonist activity of the tested compounds was evaluated on electrically stimulated
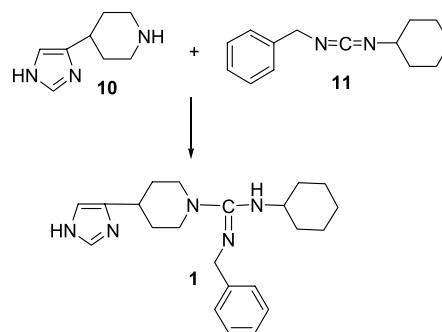
Scheme 1. Reagents and conditions: 2-methyl-2-propanol, reflux, 20 h, N_2 atmosphere.
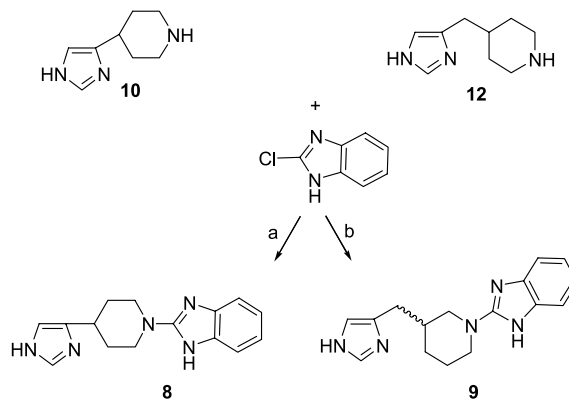
Scheme 2. Reagents and conditions: (a) DMF, 140 °C, 3 h, N_2 atmosphere; (b) 3-methyl-1-butanol, 130 °C, 18 h, N_2 atmosphere.

guinea-pig ileum, by inhibition of RAMHA-induced responses.[62]

4. Results and discussion

The present work was carried out in different phases. After the first one, consisting of the building of the rat H$_3$ receptor 3D model, two different strategies were applied to assess its ability to reproduce the SARs for H$_3$ antagonists. We first looked for a binding mode that could be applied to classical H$_3$ antagonists having strongly basic, neutral, or slightly basic polar groups and then we validated this binding hypothesis on the basis of known SARs and with the synthesis of new compounds.

The rat H$_3$ receptor model was built following standard comparative modeling procedures, described in Section 5, starting from the three-dimensional structure of bovine rhodopsin and the sequence alignment reported in Figure 2. During the homology modeling phase, the most relevant choice was to avoid the modeling of the long third intracellular loop, keeping the backbone structure of rhodopsin. The refined model was analyzed with the program PROCHECK 3.5.4[63] and resulted acceptable from a biophysical point of view, with an overall G-factor of −0.53. The Ramachandran plot reported in Figure 3 highlights the presence of only four
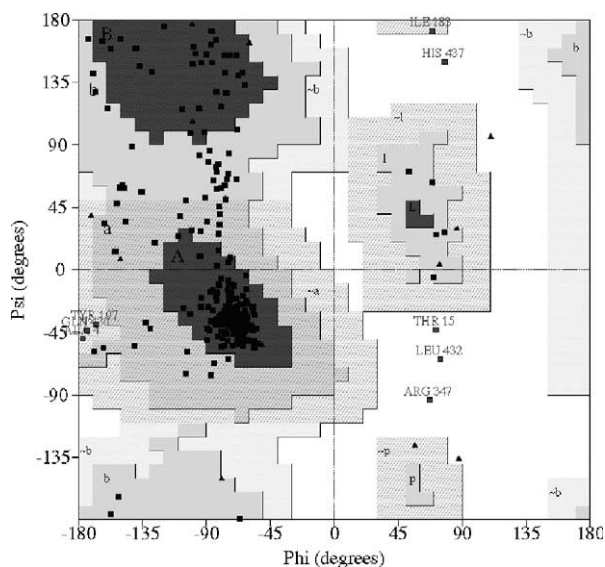
amino acids in the disallowed region: T15 in the amino terminal portion, R347 in the second intracellular loop, L432 and H437 in the carboxy terminal portion; these amino acids are positioned very far away from the putative binding site of the H$_3$ ligands.

The resulting model reveals a cavity allowing the accommodation of the agonist histamine between the charged carboxyls of E206 and D114, as suggested by sequence analysis and mutagenesis data (see Section 1). Antagonist docking started from the assumption that classical H$_3$ antagonists would share with the natural agonist the interaction between their imidazole ring and E206. This hypothesis is based on the partial structural similarity between histamine and imidazole-containing H$_3$ antagonists (i.e., the imidazole ring, the spacer, and the basic or polar portion) and on established SAR analysis.[36,64] Clobenpropit and thioperamide (Fig. 1) were the first two compounds docked within the binding site cavity. These two compounds were chosen as representatives of imidazole antagonists having a strongly basic and a neutral polar group in their side chain, respectively. Explorative runs of molecular dynamics simulations on the complexes between the receptor and the two antagonists revealed that, besides E206 and D114, two tyrosine residues, Y189 belonging to the extracellular loop 2 and Y374 in TM6, are positioned in proximity of the ligands and could participate in the interaction (Figs. 4A and B). Moreover, the two lipophilic groups,
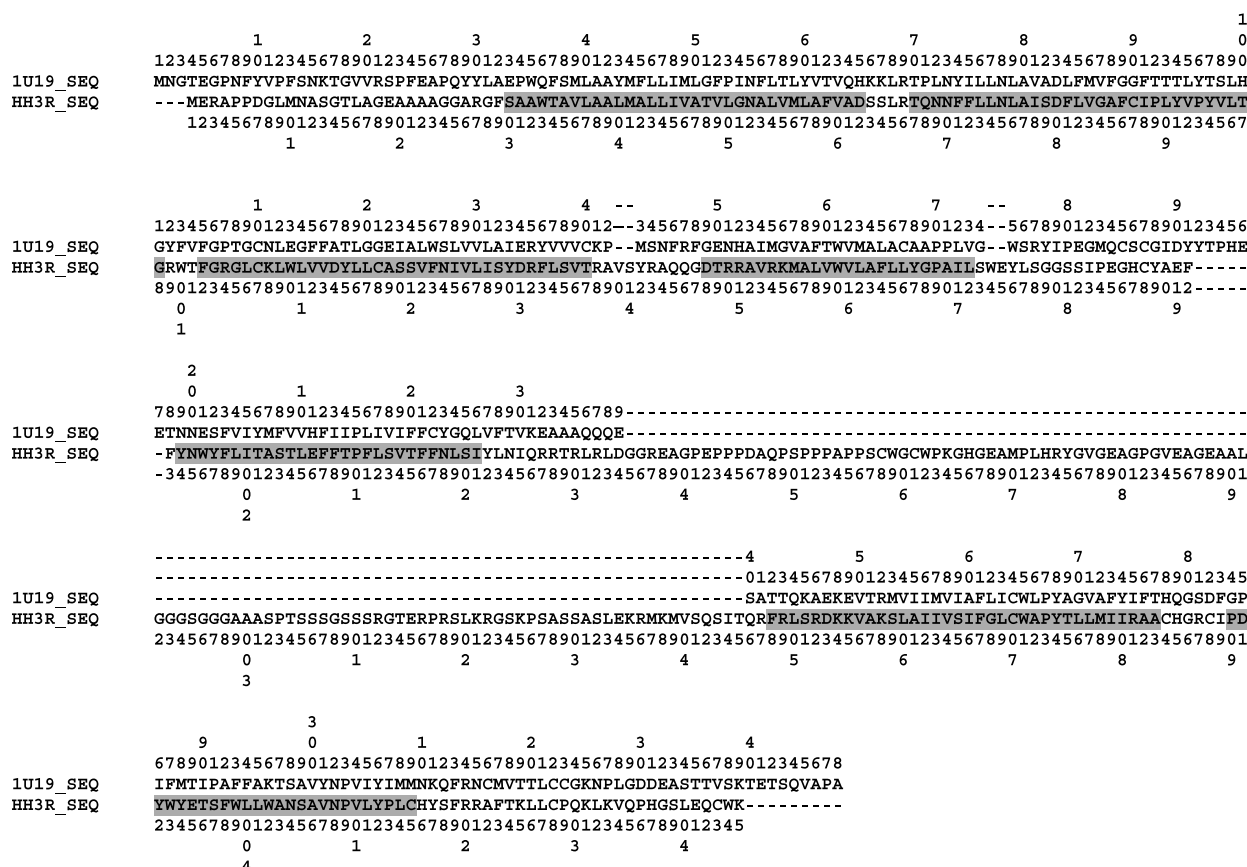
Figure 2. Sequence alignment between bovine rhodopsin and rat histamine H$_3$ receptor. Numbering of rhodopsin residues is reported in the top lines, and numbering of H$_3$ receptor amino acids in the bottom lines. The putative transmembrane domains of the H$_3$ receptor model are shaded.

Figure 3. Ramachandran plot for the H$_3$ receptor model. Amino acids in the disallowed region: T15, R347, L432, and H437.

the p-Cl-benzyl of clobenpropit and the cyclohexyl one of thioperamide, could be allocated in two different pockets, which were named P1 and P2 (Fig. 4). These pockets are mainly of lipophilic nature; the bigger one, P1, is deeply inserted between helices 3, 6, and 7 and

the p-Cl-benzyl substituent of clobenpropit is surrounded by L117, C370, W371, F367, W402, and N404. The other pocket, P2, is delimited by Y91, W110, H187, F398, W399, and W402, the last residue being at the boundary between the two pockets. The existence of a pocket corresponding to P1 had been proposed by Yao et al.[57] in their model of H$_3$ receptor; although some amino acids (i.e., C370 and N404) are common to both models, they inserted the antagonists more deeply within the pocket. A similar binding cavity had also been described in a recently reported homology model of the dopamine D$_2$ receptor.[65] The D$_2$ antagonist spiperone had been docked with the basic group close to D3.32 (corresponding to our Asp114) and its phenyl-triazaspiro[4.5]decanone substructure inserted in a region mainly composed of amino acids belonging to TM 3, 6, and 7, corresponding to many of those defining our P1 pocket. The role of this region in ligand recognition is supported by the observed changes in binding affinity deriving from mutations in adjacent amino acids (N7.43 and D2.50).

The role of the interaction between the imidazole ring and E206 is challenged by mutagenesis experiments, indicating that E206A mutation did not significantly modify the K_D value for the radioligand [^{125}I]-iodoproxyfan.[49] Iodoproxyfan, 4-[3-(4-iodo-benzyloxy)-propyl]-1H-imidazole, has only an ether oxygen as the
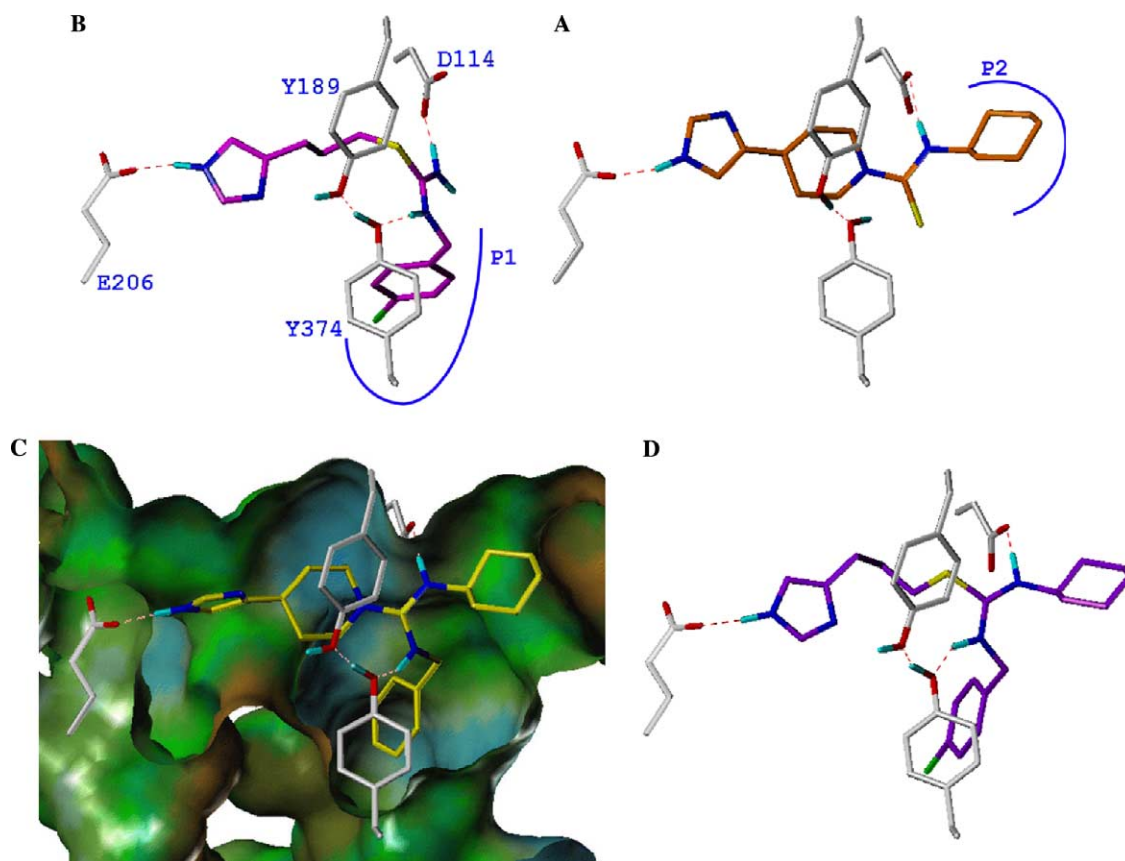
Figure 4. Energy-minimized molecular dynamics average structures of thioperamide (A, orange carbons), clobenpropit (B, magenta carbons), 1 (C, yellow carbons), and VUF5228 (D, violet carbons) within the proposed H$_3$ receptor binding site. Amino acids involved in polar interactions are represented with white carbons. Hydrogen bonds are indicated with red dotted lines. Pockets P1 and P2 are indicated by the blue lines in (A) and (B). In (C), a section of the binding site surface colored according to lipophilicity (brown: most lipophilic; blue: most hydrophilic) is also represented.

polar portion, and it is reasonable to suppose that it would hardly interact with D114 by means of this atom, possibly leading to a different binding scheme. In fact, automated docking of iodoproxyfan in our H_3 receptor model gave, besides solutions characterized by the interaction of the imidazole with E206, also different solutions, where the imidazole ring interacted with D114 and the lipophilic moiety was deeply inserted within the P1 pocket.

A superposition of clobenpropit and thioperamide similar to that resulting from these studies had been previously suggested on the basis of a pharmacophore model.[34] This had led to the synthesis of a derivative of clobenpropit with two lipophilic groups at the isothiourea moiety, resulting a potent H_3 antagonist (VUF5228, N-(4-chlorobenzyl)-N-cyclohexyl-S-[3-(4(5)-imidazolyl)- propyl]isothiourea, pK_i = 9.3).[34] This compound, having a flexible chain spacer, was docked within our H_3 receptor model and the complex was submitted to MD simulations, giving a pattern of interactions similar to those of clobenpropit and thioperamide. The imidazole ring interacted with E206, while the charged isothiourea was hydrogen-bonded to D114 and Y374; the p-Cl-benzyl and the cyclohexyl substituents were positioned within the P1 and P2 pockets, respectively (Fig. 4D). As no conformationally constrained compounds directly deriving from the superposition of clobenpropit and thioperamide have been described, we prepared compound **1**, in which the rigid imidazolyl-piperidine scaffold of thioperamide carries a basic guanidine group, substituted by a cyclohexyl and a benzyl group attached to different nitrogens (Fig. 1). This compound revealed a good affinity for rat H_3 receptors (pK_i = 8.02, Table 2), and the limited pK_i reduction, with respect to clobenpropit and thioperamide (pK_i = 9.32[66] and 8.59,[67] respectively) led us to the conclusion that the binding site could actually accommodate two bulky lipophilic substituents linked to the central basic polar group in the conformation supposed by the pharmacophore model described by De Esch et al. and confirmed by our conformationally constrained derivative.

Compound **1** was docked within the H_3 receptor model; the position of the ligand and the whole pattern of interactions were maintained during 1 ns MD simulation performed on the complex (Fig. 5). The interaction of **1** with the H_3 receptor consisted of a hydrogen bond between the imidazole ring and the carboxyl group of E206
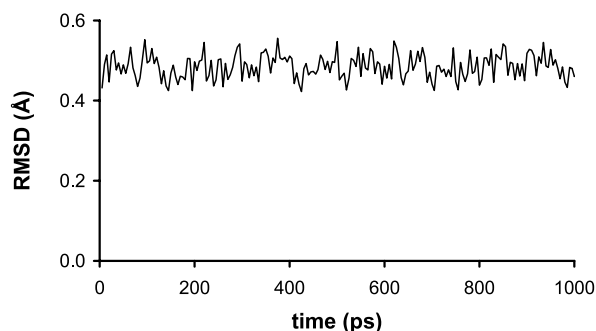
Figure 5. Root mean square distances (RMSD) calculated for compound **1** and the H_3 receptor residues within a sphere of 6 Å around the ligand, during 1 ns MD simulation, after an equilibration time of 100 ps.

and of two additional hydrogen bonds taken by the guanidine group with D114 and Y374 (Fig. 4C). In its cationic state, the guanidinium fragment acted as a hydrogen bond donor toward the oxygen of Y374. Even if electron delocalization reduces the ability of phenolic oxygens to receive hydrogen bonds, the occurrence of this kind of interaction is supported by some cases observed in the PDB[68] (PDB IDs: 1KZJ, 1MCH, 1N1M, 1HSB). It is also worth noting that Y374 is conserved among the histamine receptors and it is spatially close to W371, the tryptophan residue supposed to be involved in receptor activation;[40,41] this interaction could therefore be critical for the antagonist behavior of these ligands. In analogy with the results obtained for clobenpropit and thioperamide, the tyrosine residue Y189 remains close to the ligand without interacting with it, but forming a hydrogen bond with the other tyrosine Y374. As expected from the superposition of clobenpropit and thioperamide, the two lipophilic groups (i.e., the benzyl and the cyclohexyl ones) occupied the two pockets P1 and P2, respectively. Compound **1** was also docked within the H_3 receptor by means of an automatic docking procedure, looking for possible alternative dispositions. Among the solutions with high estimated binding energy, three main clusters were obtained, in which the imidazole ring, besides the accommodation in proximity of E206, was positioned in the two pockets P1 and P2. These alternative solutions resulted not stable when submitted to geometry optimization and MD simulations, loosing some of their polar interactions.

After the identification of the aforementioned binding site, several classic H_3 antagonists were successfully docked and submitted to MD simulations (e.g., cipralisant and derivatives, ciproxifan, and imoproxifan) giving solutions consistent with the proposed binding scheme (data not shown). The ability of this model to reproduce SARs was deeply investigated considering a series of potent H_3 antagonists having a flexible chain and a 2-aminobenzimidazole moiety.[38,39] An interesting SAR profile had been previously reported for these compounds (see Section 1 and Table 1): while for derivatives with shorter chain (**2–4**) the methylation of the exocyclic nitrogen led to a decrease in affinity and the methylation of the endocyclic one to an increase in potency, the opposite was observed for compounds with longer chain

Table 2. H_3 receptor affinity and antagonist potency of newly synthesized compounds

Compound	pK_i[a,b]	pK_b[b,c]
1	8.02 ± 0.12	8.83 ± 0.12
8	7.13 ± 0.09	8.22 ± 0.09
9	7.81 ± 0.02	8.53 ± 0.12

[a] Inhibition of [³H]RAMHA-specific binding to rat cerebral cortex membranes.
[b] Means ± SEM of four independent determinations.
[c] Antagonism of RAMHA-induced inhibition of twitch response of guinea-pig isolated ileum. pK_b values were obtained according to Furchgott's method.[73]

(**5–7**), which showed the highest potency for the parent (**5**) and the 2-*N*-methylamino derivative (**6**). Docking and MD simulations provided an interpretation of these SARs. The two parent compounds **2** and **5** were docked into the binding site, arranging the imidazole ring between E206 and Y189, and the 2-aminobenzimidazole group close to D114 and Y374. The two complexes were submitted to MD simulations and the energy-minimized average structures obtained from 30 representative snapshots of MD trajectory are represented in Figure 6A. The imidazole rings interact not only with the carboxyl group of E206 but also with the hydroxyl function of Y189. This interaction pattern is comparable to that found for the imidazole ring in the crystal structure of histamine bound to female-specific histamine binding protein (PDB ID: 1QFT).[69] On the basis of the analysis of the structure of bovine rhodopsin bound to retinal and of mutagenesis data from aminergic receptors, a role of EL2 in the definition of the binding site of aminergic receptors has been recognized. In particular, the amino acids immediately following the conserved cysteine residue in EL2 (i.e., Y189 in the H_3 receptor) were defined as potentially able to face the binding site.[70] However, the supposed role of these amino acids in H_3 antagonist binding is far from being demonstrated. In fact, no experimental data have been reported about its importance in antagonist binding, and thioperamide binds with comparable potencies to H_3 and H_4 receptor, where Y189 is replaced by a glutamic acid.[71] These observations, and the fact that a direct interaction was only observed in the MD runs for 2-aminobenzimidazole derivatives, do not support a crucial role for this residue.

While the imidazole rings of the two compounds maintained the original polar interactions, the benzimidazole moieties showed different arrangements, influenced by the different length of the polymethylene chain. In fact, the more potent compound **5** was able to interact with both D114, through its endocyclic NH, and Y374, accepting a hydrogen bond through the other benzimidazole nitrogen; on the contrary, the shorter compound **2** gave a different arrangement, placing its benzimidazole nucleus into the lipophilic pocket P1. This resulted in worse polar interactions, as illustrated by the sum of the distances between the four couples of atoms involved in polar interactions: 10.93 ± 0.27 Å for compound **5** and 13.16 ± 0.86 Å for compound **2**, evidencing both a longer mean value and wider oscillations for compound **2**; this could be related to

the different affinity of the two compounds. Docking and MD simulations on the methylated derivatives gave results consistent with the data reported in Table 1. In fact, while for the longer compounds only methylation of the exocyclic nitrogen was allowed to preserve polar interactions, N-methylation of the benzimidazole in the shorter series led to a better steric arrangement which, in the absence of strong polar interactions, could be responsible for the small increase of affinity observed for compound **4** over **2** (Fig. 6B).

To further evaluate the stability of the ligand–receptor interactions, MD simulations were performed for the complexes between the H_3 receptor and compounds **1**, **2**, and **5** with mobile protein backbone, applying only constraints necessary to maintain the starting tertiary structure of the protein. No relevant differences from the previously described ligand–receptor interactions were observed, except for the slightly greater mobility of the ligands. In particular, the sum of the distances between interacting groups increased more for the less potent compound, **2** (16.54 ± 0.88 Å), than for the more potent one, **5** (11.21 ± 0.37 Å).

To finally validate our model, we prepared two new benzimidazole derivatives with limited conformational freedom. We observed that the conformation of the three-methylene chain in the putative active form of **5** (Fig. 6A) resembled the shape of a piperidine ring. The imidazole ring and the attached methylene group occupied the space of a 3-equatorial substituent on this hypothetical ring. Compounds **8** and **9** (Fig. 7) were therefore synthesized and tested, having predicted a better fit of the H_3 receptor binding site for **9**. As expected, the second compound showed higher affinity than the first (**8**: $pK_i = 7.13$, (±)**9**: $pK_i = 7.81$), even if it was less
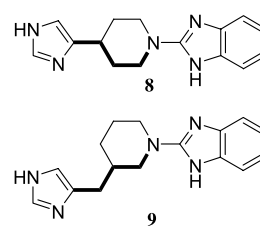
Figure 7. Newly synthesized H_3 antagonists, **8** and **9**, with limited conformational freedom.
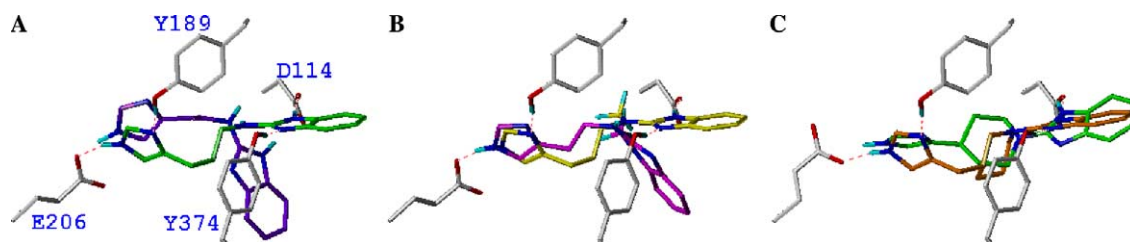
Figure 6. Energy-minimized molecular dynamics average structures of compounds **2** and **5** (A, violet and green carbons, respectively), compounds **4** and **6** (B, magenta and yellow carbons, respectively), and compounds **8** and **9** (C, green and orange carbons, respectively) in the H_3 receptor binding site. Amino acids involved in polar interactions are represented with white carbons. Hydrogen bonds are indicated with red dotted lines.

potent than the corresponding open compound **6** (pK_i = 8.6.0). The pharmacological characterization of the newly synthesized compounds **1**, **8**, and **9** is reported in detail in Table 2. The limited, but significant drop of pK_i could be due to the fact that the racemate of **9** was tested, or to an unfavorable steric effect of the piperidine ring, but it is our opinion that only qualitative, yet useful, indications can be expected from approximate models like the one presented here. Docking and MD simulations revealed that **9** was able to undertake the same pattern of interactions as the other 2-aminobenzimidazole derivatives and also **8** could be accommodated in the binding site in a good arrangement (Fig. 6C); however, the mean value of the distances describing polar interactions with the amino acids of the binding site was lower for compound **9**, in accordance with its higher experimental affinity. No quantitative structure–activity relationship was sought for the distances between interacting groups and the potency of the compounds, because of the approximations in model building and the low number of degrees of freedom.

Two models of the rat H_3 receptor have previously been published, in which H_3 receptor antagonists had been docked. The position of our putative binding site is similar to that presented in the work by Stark et al.,[56] but the interaction between the imidazole ring and the receptor is quite different. In that model the imidazole ring interacts with two acidic residues (E206 and E191), while in the present model it interacts with an acidic amino acid and a tyrosine residue. In our model, D114 interacts with the polar portion of all the H_3 antagonists under investigation; in the model proposed by Stark et al. the bulky cyclohexyl ring of thioperamide prevents the interaction between D114 and its thiourea group. In the second H_3 receptor model, reported by Yao et al.,[57] both agonists and antagonists have been placed within the P1 pocket, in an arrangement completely different from that proposed here.

In conclusion, a model of the H_3 receptor is presented, with its validation through the analysis of SARs for classical H_3 antagonists and the synthesis of new compounds. The ability of this model to explain and predict structure–activity profiles for a series of classical H_3 antagonists resulted satisfactory on a qualitative scale; the high flexibility of the model implies that different solutions can be found, and the consideration of average conformations from stabilized MD simulation helps in the evaluation of new ligand structures.

5. Experimental

5.1. Chemistry

5.1.1. General methods. Melting points of intermediates and final compounds were not corrected, and were determined with a Büchi instrument (Tottoli) and with Gallenkamp melting point apparatus. The final compounds were analyzed for C, H, and N: the percentages we found were within ±0.4 of the theoretical values. ^{1}H NMR spectra were recorded on a Bruker 300

spectro-meter (at 300.13 MHz); chemical shifts (δ scale) are reported in parts per million (ppm) relative to the central peak of the solvent. ^{1}H NMR spectra are reported in order: multiplicity and number of protons. Abbreviations are the following: Im, imidazolyl; Bz, benzimidazolyl; Pip, piperidyl. Mass spectra were recorded using a Finnigan MAT SSQ 710 instrument. Reactions were monitored by TLC, on Kieselgel 60 F 254 (DC-Alufolien, Merck). Final compounds and intermediates were purified by chromatography on preparative Gilson MPLC, using a SiO_2 column (MN-Kieselgel 25–40 μm Macherey-Nagel). Abbreviations for solvents are the following: Et$_2$O, diethyl ether; DCM, dichloromethane; EtOH, ethanol; DMF, dimethyl formamide.

5.1.2. *N*-Benzyl-*N'*-cyclohexyl-4-(1*H*-imidazol-4-yl)-piperidine-1-carboxamidine dioxalate (1 · 2C$_2$H$_2$O$_4$). A solution of 1.05 mmol (0.24 g) of benzyl-cyclohexyl-carbodiimide (**11**) and 1.25 mmol (0.19 g) of 4-(1*H*-imidazol-4-yl)-piperidine (**10**) in 1 ml of 2-methyl-2-propanol was heated at reflux temperature for 20 h under nitrogen atmosphere. The solvent was evaporated under reduced pressure and the crude product was purified by column chromatography [SiO$_2$ methanol (NH$_3$ 5% w/w)]. The free base was treated with a saturated ethanolic solution of oxalic acid to yield 0.40 mmol (0.22 g, 38%) of dioxalate of **1**, after crystallization from EtOH abs/Et$_2$O. Mp 197–198 °C dec.

^{1}H NMR (DMSO-d_6): δ 1.00–1.27 ppm (m, 5H), 1.52–1.75 (m, 7H), 2.00 (d, 2H), 2.91 (s, 1H), 3.16–3.24 (t, 3H), 3.68 (d, 2H), 4.41 (d, 2H, CH$_2$), 7.07 (s, 1H, Im-5-H), 7.29–7.43 (m, 5H, Benzyl), 7.57 (d, 1H), 8.16 (s, 1H, Im-2-H). MS (CI) 366 [M+1]$^+$. Anal. (C$_{22}$H$_{31}$N$_5$ · 2C$_2$H$_2$O$_4$ · 1/2 H$_2$O) C, H, N.

5.1.3. 2-[4-(1*H*-Imidazol-4-yl)-piperidin-1-yl]-1*H*-benzimidazole dihydrochloride (8 · 2HCl). A solution containing 2.98 mmol (0.45 g) of 4-(1*H*-imidazol-4-yl)-piperidine (**10**) and 1.97 mmol (0.30 g) of 2-chlorobenzimidazole in 3 ml of DMF was heated at 140 °C for 3 h under nitrogen atmosphere. The reaction mixture was then treated with aqueous sodium carbonate and extracted with ethyl acetate. The organic layer was dried over sodium sulfate and evaporated under reduced pressure. The crude product was purified by column chromatography (SiO$_2$ dichloromethane/methanol (NH$_3$ 5% w/w)/methanol 100:2:8).

The free base was treated with EtOH saturated with HCl to yield 0.58 mmol (0.20 g, 29%) dihydrochloride of **8**, after crystallization from EtOH abs/Et$_2$O. Mp 260 °C dec.

^{1}H NMR (DMSO-d_6) δ 1.68–1.81 (m, 2H, Pip), 2.10 (d, 2H, Pip), 3.12 (t, 1H, Pip), 3.42 (t, 2H, Pip), 4.32 (d, 2H, Pip), 7.24–7.27 (m, 2H, Bz), 7.36–7.40 (m, 2H, Bz), 7.48 (s, 1H, Im-5-H), 8.77 (s, 1H, Im-2-H). MS (CI) 268 [M+1]$^+$. Anal. (C$_{15}$H$_{17}$N$_5$ · 2HCl · H$_2$O) C, H, N.

5.1.4. 2-[3-(1*H*-Imidazol-4-ylmethyl)-piperidin-1-yl]-1*H*-benzimidazole dihydrochloride (9 · 2HCl). A mixture containing 1.53 mmol (0.50 g) of 3-(1*H*-imidazol-4-ylmeth-

yl)-piperidine (**12**) and 0.77 mmol (0.12 g) of 2-chlorobenzimidazole was added to 5 ml of 3-methyl-1-butanol and heated at 130 °C for 18 h under nitrogen atmosphere. The reaction mixture was then treated with diethyl ether and the resulting precipitate was filtered off and purified by column chromatography (SiO$_2$ dichloromethane/methanol (NH$_3$ 5% w/w) 20:1).

The free base was treated with EtOH saturated with HCl yielding 0.45 mmol (0.16 g, 60%) dihydrochloride of **9**, after crystallization from EtOH abs/Et$_2$O. Mp 188–190 °C.

^{1}H NMR (DMSO-d_6) δ 1.25–1.3 (m, 1H, Pip), 1.52-1.57 (m, 1H, Pip), 1.72–1.83 (m, 2H, Pip), 2.00 (s, 1H, Pip), 2.59–2.76 (m, 2H, Pip), 3.08 (t, 1H, Pip), 3.27 (t, 1H, Pip), 3.81 (d, 2H, CH$_2$), 7.23–7.26 (m, 2H, Ph), 7.34–7.36 (m, 2H, Ph + Im-5-H), 8.80 (s, 1H, Im-2-H). MS (CI) 282 [M+1]$^+$. Anal. (C$_{16}$H$_{19}$N$_5$ · 2HCl · EtOH) C, H, N.

5.2. Pharmacology

5.2.1. Binding assays. Rat (Wistar) cerebral cortex membranes were incubated for 30 min with [^{3}H]RAMHA 0.5 nM and the compounds were studied (1 nM–10 µM), in Tris–HCl 50 mM, pH 7.4, NaCl 50 mM, EDTA 0.5 mM and rapidly filtered under vacuum (AAWP Millipore filters 0.8 µm). Specific binding was defined as the binding inhibited by thioperamide 10 µM, and the pK_i values were calculated from the IC$_{50}$ values estimated in displacement curves of the compounds tested versus 0.5 nM [^{3}H]RAMHA according to Cheng–Prusoff's equation.[72]

5.2.2. Functional assays. Portions of guinea-pig ileum were mounted on a coaxial platinum electrode assembly in a 10 ml water-jacketed organ bath containing Krebs–Henseleit solution aerated with 95% O$_2$–5% CO$_2$ and maintained at 37 °C. Single electrical pulses were delivered to the tissue (0.1 Hz, 1 ms, 20–40 mA) from a stimulator (LACE Elettronica Model ES-3, Ospedaletto PI, Italy). Cumulative concentration–response curves for the inhibition of electrically stimulated contractions were determined for the H$_3$ selective agonist RAMHA (1 nM–1 µM). The tissues were allowed to equilibrate with the compounds under study (1 nM–10 µM) for 30 min before the generation of concentration–response curves to the agonist. pK_b values ('apparent pA_2') were determined according to Furchgott's equation.[73]

5.3. Model building and molecular modeling

The initial alignment between the amino acid sequences of bovine rhodopsin (BR) (Swiss-Prot ID P02699) and rat histamine H$_3$ receptor (Swiss-Prot ID Q9QYN8) was performed using the program ClustalW,[74] with PAM250[75] scoring matrix, opening gap penalty of 10, end gap penalty of 10, extending gap penalty of 0.05, and separation gap penalty of 0.05. The alignment was inspected and modified in the region of the second extracellular loop to allow the formation of a disulfide bond between the two cysteines C107 in TM3 and C188 in EL2. The final alignment is reported in Figure 2.

The high-resolution crystallographic coordinates of BR (PDB ID 1U19)[42] were taken from the RCSB Protein Data Bank.[68] Employing the *Biopolymer* module of Sybyl 6.8 software,[76] the amino acids in the transmembrane (TM) regions of BR were mutated to those of the rat H$_3$ receptor, and the loop regions were inserted by the *Protein Loop Search* procedure. The long third intracellular loop of the H$_3$ receptor was not modeled; the backbone of BR loop was maintained, replacing the amino acid side chains with those of the corresponding amino acids in the H$_3$ receptor. The model of the H$_3$ receptor was submitted to geometry optimization with the MMFF94s force field[77] implemented in Sybyl, with a dielectric constant of 1 and a non-bonded cutoff of 8 Å, applying a stepwise procedure. Initially, the backbone of the TMs was kept fixed, while the backbone of other regions and all the side chains were submitted to 20,000 steps of energy minimization employing the Powell method.[78] Distance constraints were then introduced between the backbone atoms of the TMs involved in hydrogen bonds, and the whole structure was energy minimized for three runs of 20,000 steps each, gradually reducing the force constant of the constraints (100, 50, and 25 kcal/(mol Å^2), respectively). In a fourth run, the constraints were removed and the receptor was fully minimized to a gradient of 0.02 kcal/(mol Å).

Ligand structures were built by the standard sketch options of Sybyl and they were submitted to geometry optimization with MMFF94s force field to a gradient of 0.01 kcal/(mol Å) before the docking procedure. Clobenpropit, VUF5228, and compound **1** were considered protonated at the isothiourea or guanidine group. Ligands were merged into the putative binding site, allowing the imidazole ring to interact with E206 and the polar group with D114. The N^τ–H tautomer of the neutral imidazole ring was considered for all ligands, being the one able to interact with the carboxyl function of E206. The ligand accommodation was refined by 100 steps of the *Dock Minimize* procedure in Sybyl with the MMFF94s force field; the geometry of the ligand–receptor complexes was then optimized to a gradient of 0.05 kcal/(mol Å), keeping the position of the protein backbone atoms fixed.

Besides the interactive docking procedure, the program AutoDock 3.0.5[79] was employed to dock the antagonist **1** into the receptor binding site, starting from a minimum energy conformation placed in an arbitrary orientation. A grid of 80 × 80 × 80 points with 0.375 Å of spacing interval, centered on the carboxyl carbon of D114 was chosen, and docking solutions were searched applying a genetic algorithm–local search procedure, with standard parameters.[80] The 100 solutions obtained were ranked and clustered on the basis of their estimated binding energy, as calculated by AutoDock.

Molecular dynamics simulations were performed with Macromodel 8.0,[81] employing the MMFF94 force field with a time step of 1.5 fs, a dielectric constant of 1 and a non-bonded cutoff of 8 Å, keeping fixed the position of the backbone atoms. Starting from minimum energy conformations of the receptor-ligand complexes,

the temperature was gradually raised to 310 K during an equilibration period of 100 ps and it was maintained for 1 ns, collecting 200 snapshots every 5 ps. The average structures obtained from 30 representative snapshots of MD trajectory were energy minimized with the MMFF94s force field to a gradient of 0.05 kcal/(mol Å), with fixed protein backbone.

For the complexes between the H_3 receptor and compounds **1**, **2**, and **5** MD simulations were also performed with mobile protein backbone atoms. Distance constraints were applied between the backbone N and O atoms of TM regions involved in hydrogen bonds, with a force constant of 500 kJ/(mol Å^2) and a tolerance of 0.3 Å to keep the α-helix secondary structure, and a position constraint was introduced for all the backbone atoms, with a low force constant of 50 kJ/(mol Å^2) and a tolerance of 1.0 Å.

During MD simulations, at each snapshot, the sum of four distances between interacting groups of the H_3 receptor and the ligand was monitored: (1) the distance between the carboxyl oxygen of E206 and N^τ of the imidazole ring; (2) the distance between the oxygen of Y189 and N^π of the imidazole ring; (3) the distance between the carboxyl oxygen of D114 and the endocyclic NH of the benzimidazole ring; and (4) the distance between the oxygen of Y374 and the N atom of the benzimidazole ring.

Supplementary data

Supplementary data associated with this article can be found, in the online version, at doi:10.1016/j.bmc.2005.05.072.

References and notes

1. Hill, S. J.; Ganellin, C. R.; Timmerman, H.; Schwartz, J.-C.; Shankley, N. P.; Young, J. M.; Schunack, W.; Levi, R.; Hass, H. L. *Pharmacol. Rev.* **1997**, *49*, 253.
2. Nakamura, T.; Itadani, H.; Hidaka, Y.; Ohta, M.; Tanaka, K. *Biochem. Biophys. Res. Commun.* **2000**, *279*, 615.
3. Oda, T.; Morikawa, N.; Saito, Y.; Masuho, Y.; Matsumoto, S. *J. Biol. Chem.* **2000**, *275*, 36781.
4. Arrang, J.-M.; Garbarg, M.; Schwartz, J.-C. *Nature* **1983**, *302*, 832.
5. Arrang, J.-M.; Garbarg, M.; Schwartz, J.-C. *Neuroscience* **1985**, *15*, 553.
6. Arrang, J.-M.; Drutel, G.; Schwartz, J.-C. *Br. J. Pharmacol.* **1995**, *114*, 1518.
7. Schlicker, E.; Betz, R.; Göthert, M. *Naunyn-Schmiedeberg's Arch. Pharmacol.* **1988**, *337*, 588.
8. Schlicker, E.; Fink, K.; Hinterthaner, M.; Göthert, M. *Naunyn-Schmiedeberg's Arch. Pharmacol.* **1989**, *340*, 633.
9. Schlicker, E.; Fink, K.; Detzner, M.; Göthert, M. *J. Neural Transm.* **1993**, *93*, 1.
10. Leurs, R.; Blandina, P.; Tedford, C.; Timmerman, H. *Trends Pharmacol. Sci.* **1998**, *19*, 177.
11. Stark, H.; Arrang, J.-M.; Ligneau, X.; Garbarg, M.; Ganellin, C. R.; Schwartz, J.-C.; Schunack, W. In King, F. D., Oxford, A. W., Eds.; Progress in Medicinal Chemistry; Elsevier: Amsterdam, 2001; Vol. 38, pp 279–308.
12. Witkin, J. M.; Nelson, D. L. *Pharmacol. Ther.* **2004**, *103*, 1.
13. Glase, S. A.; Robertson, D. W.; Wise, L. D. *Annu. Rep. Med. Chem.* **2002**, *37*, 11.
14. Vohora, D.; Pal, S. N.; Pillai, K. K. *Pharmacol. Biochem. Behav.* **2001**, *68*, 735.
15. Yoshimatsu, H.; Itateyama, E.; Kondou, S.; Tajima, D.; Himeno, K.; Hidaka, S.; Kurokawa, M.; Sakata, T. *Diabetes* **1999**, *48*, 2286.
16. Stark, H.; Ligneau, X.; Arrang, J.-M.; Schwartz, J.-C.; Schunack, W. *Bioorg. Med. Chem. Lett.* **1998**, *8*, 2011.
17. Leurs, R.; Vollinga, R. C.; Timmerman, H. *Prog. Drug Res.* **1995**, *45*, 107.
18. Ganellin, C. R.; Hosseini, S. K.; Khalaf, Y. S.; Tertiuk, W.; Arrang, J.-M.; Garbarg, M.; Ligneau, X.; Schwartz, J.-C. *J. Med. Chem.* **1995**, *38*, 3342.
19. Clitherow, J. W.; Beswick, P.; Irving, W. J.; Scopes, D. I. C.; Barnes, J. C.; Clapham, J.; Brown, J. D.; Evans, D. J.; Hayes, A. G. *Bioorg. Med. Chem. Lett.* **1996**, *6*, 833.
20. Mor, M.; Bordi, F.; Silva, C.; Rivara, S.; Crivori, P.; Plazzi, P. V.; Ballabeni, V.; Caretta, A.; Barocelli, E.; Impicciatore, M.; Carrupt, P.-A.; Testa, B. *J. Med. Chem.* **1997**, *40*, 2571.
21. Mor, M.; Bordi, F.; Silva, C.; Rivara, S.; Zuliani, V.; Vacondio, F.; Morini, G.; Barocelli, E.; Ballabeni, V.; Impicciatore, M.; Plazzi, P. V. *Farmaco* **2000**, *55*, 27.
22. Plazzi, P. V.; Bordi, F.; Mor, M.; Silva, C.; Morini, G.; Caretta, A.; Barocelli, E.; Vitali, T. *Eur. J. Med. Chem.* **1995**, *30*, 881.
23. Bordi, F.; Mor, M.; Morini, G.; Plazzi, P. V.; Silva, C.; Carretta, A. *Farmaco* **1994**, *49*, 153.
24. Plazzi, P. V.; Mor, M.; Bordi, F.; Silva, C.; Rivara, S.; Caretta, A.; Ballabeni, V.; Impicciatore, M.; Vitali, T. *Farmaco* **1997**, *52*, 295.
25. Tedford, C. E.; Phillips, J. G.; Gregory, R.; Pawloski, G. P.; Fadnis, L.; Khan, M. A.; Ali, S. M.; Handley, M. K.; Yates, S. L. *J. Pharmacol. Exp. Ther.* **1999**, *289*, 1160.
26. Arrang, J.-M.; Garbarg, M.; Lancelot, J.-C.; Lecomte, J.-M.; Pollard, H.; Robba, M.; Schunack, W.; Schwartz, J.-C. *Nature* **1987**, *327*, 117.
27. Van der Goot, H.; Schepers, M. J. P.; Sterk, G. J.; Timmerman, H. *Eur. J. Med. Chem.* **1992**, *27*, 511.
28. Chai, W.; Breitenbucher, J. G.; Kwok, A.; Li, X.; Wong, V.; Carruthers, N. I.; Lovenberg, T. W.; Mazur, C.; Wilson, S. J.; Axe, F. U.; Jones, T. K. *Bioorg. Med. Chem. Lett.* **2003**, *13*, 1767.
29. Zaragoza, F.; Stephensen, H.; Knudsen, S. N.; Pridal, L.; Wulff, B. S.; Rimvall, K. *J. Med. Chem.* **2004**, *47*, 2833.
30. Mikó, T.; Ligneau, X.; Pertz, H. H.; Ganellin, R.; Arrang, J.-M.; Schwartz, J.-C.; Schunack, W.; Stark, H. *J. Med. Chem.* **2003**, *46*, 1523.
31. Faghih, R.; Dwight, W.; Pan, J. B.; Fox, G. B.; Krueger, K. M.; Esbenshade, T. A.; McVey, J. M.; Marsh, K.; Bennani, Y. L.; Hancock, A. A. *Bioorg. Med. Chem. Lett.* **2003**, *13*, 1325.
32. Apodaca, R.; Dvorack, C. A.; Xiao, W.; Barbier, A. J.; Boggs, J. D.; Wilson, S. J.; Lovenberg, T.; Carruthers, N. I. *J. Med. Chem.* **2003**, *46*, 3938.

33. Stark, H. *Expert Opin. Ther. Patent* **2003**, *13*, 851.
34. De Esch, I. J. P.; Mills, J. E. J.; Perkins, T. D. J.; Romeo, G.; Hoffmann, M.; Wieland, K.; Leurs, R.; Menge, W. M. P. B.; Nederkoorn, P. H. J.; Dean, P. M.; Timmerman, H. *J. Med. Chem.* **2001**, *44*, 1666.
35. Rivara, S.; Mor, M.; Bordi, F.; Silva, C.; Zuliani, V.; Vacondio, F.; Morini, G.; Plazzi, P. V.; Carrupt, P.-A.; Testa, B. *Drug Des. Discov.* **2003**, *18*, 65.
36. De Esch, I. J. P.; Timmerman, H.; Menge, W. M. P. B.; Nederkoorn, P. H. J. *Arch. Pharm. Pharm. Med. Chem.* **2000**, *333*, 254.
37. Windhorst, A. D.; Timmerman, H.; Worthington, E. A.; Bijloo, G. J.; Nederkoorn, P. H. J.; Menge, W. M. P. B.; Leurs, R.; Herscheid, J. D. M. *J. Med. Chem.* **2000**, *43*, 1754.
38. Mor, M.; Bordi, F.; Silva, C.; Rivara, S.; Zuliani, V.; Vacondio, F.; Rivara, M.; Barocelli, E.; Bertoni, S.; Ballabeni, V.; Magnanini, F.; Impicciatore, M.; Plazzi, P. V. *Bioorg. Med. Chem.* **2004**, *12*, 663.
39. Zuliani, V.; Bordi, F.; Rivara, M.; Silva, C.; Vacondio, F.; Morini, G.; Rivara, S.; Barocelli, E.; Ballabeni, V.; Bertoni, S.; Magnanini, F.; Plazzi, P. V. *Farmaco* **2003**, *58*, 891.
40. Ballesteros, J. A.; Weinstein, H. *Methods Neurosci.* **1995**, *25*, 366.
41. Visiers, I.; Ballesteros, J. A.; Weinstein, H. *Methods Enzymol.* **2002**, *343*, 329.
42. Okada, T.; Sugihara, M.; Bondar, A.-N.; Elstner, M.; Entel, P.; Buss, V. *J. Mol. Biol.* **2004**, *342*, 571.
43. Ballesteros, J. A.; Jensen, A. D.; Liapakis, G.; Rasmussen, S. G. F.; Shi, L.; Gether, U.; Javitch, J. A. *J. Biol. Chem.* **2001**, *276*, 29171.
44. Moro, S.; Jacobson, K. A. *Curr. Pharm. Des.* **2002**, *8*, 2401.
45. Archer, E.; Maigret, B.; Escurieut, C.; Pradayrol, L.; Fourmy, D. *Trends Pharmacol. Sci.* **2003**, *24*, 36.
46. Oliveira, L.; Paiva, A. C. M.; Vriend, G. *J. Comput. Aided Mol. Des.* **1993**, *7*, 649.
47. Strader, C. D.; Sigal, I. S.; Candelore, M. R.; Rands, E.; Hill, W. S.; Dixon, R. A. F. *J. Biol. Chem.* **1988**, *263*, 10267.
48. Horn, F.; Vriend, G.; Cohen, F. E. *Nucleic Acids Res.* **2001**, *29*, 346.
49. Uveges, A. J.; Kowal, D.; Zhang, Y.; Spangler, T. B.; Dunlop, J.; Semus, S.; Jones, P. G. *J. Pharmacol. Exp. Ther.* **2002**, *301*, 451.
50. Gantz, I.; DelValle, J.; Wang, L.; Tashiro, T.; Munzert, G.; Guo, Y.-J.; Konda, Y.; Yamada, T. *J. Biol. Chem.* **1992**, *267*, 20840.
51. Otha, K.; Hayashi, H.; Mizuguchi, H.; Kagamiyama, H.; Fujimoto, K.; Fukui, H. *Biochem. Biophys. Res. Commun.* **1994**, *203*, 1096.
52. Leurs, R.; Smit, M. J.; Tensen, C. P.; Terlaak, A. M.; Timmerman, H. *Biochem. Biophys. Res. Commun.* **1994**, *201*, 295.
53. Moguilevsky, N.; Varsalona, F.; Guillaume, J. P.; Noyer, M.; Gillard, M.; Daliers, J.; Henichart, J. P.; Bollen, A. *J. Recept. Signal Transduc. Res.* **1995**, *15*, 91.
54. Strader, C. D.; Candelore, M. R.; Hill, W. S.; Sigal, I. S.; Dixon, R. A. *J. Biol. Chem.* **1989**, *264*, 13572–13578.
55. Shin, N.; Coates, E.; Murgolo, N. J.; Morse, K. L.; Bayne, M.; Strader, C. D.; Monsma, F. J., Jr. *Mol. Pharmacol.* **2004**, *62*, 38.
56. Stark, H.; Sippl, W.; Ligneau, X.; Arrang, J.-M.; Ganellin, C. R.; Schwartz, J.-C.; Schunack, W. *Bioorg. Med. Chem. Lett.* **2001**, *11*, 951.
57. Yao, B. B.; Hutchins, C. W.; Carr, T. L.; Cassar, S.; Masters, J. N.; Bennani, Y. L.; Esbenshade, T. A.; Hancock, A. A. *Neuropharmacology* **2003**, *44*, 773.
58. Windhorst, A. D.; Timmerman, H.; Worthington, E. A.; Bijloo, G. J.; Nederkoorn, P. H. J.; Menge, W. M. P. B.; Leurs, R.; Hersch, J. D. M. *J. Med. Chem.* **2000**, *43*, 1754.
59. Jaszay, Z. M.; Petnehazy, I.; Toke, L.; Szajani, B. *Synthesis* **1987**, *5*, 520.
60. Liu, Q.; Luedtke, N. W.; Tor, Y. *Tetrahedron Lett.* **2001**, *42*, 1445.
61. Vollinga, R. C.; de Koning, J. P.; Jansen, F. P.; Leurs, R.; Menge, W. M. P. B.; Timmerman, H. *J. Med. Chem.* **1994**, *37*, 332.
62. Barocelli, E.; Ballabeni, V.; Caretta, A.; Bordi, F.; Silva, C.; Morini, G.; Impicciatore, M. *Agents Actions* **1993**, *38*, 158.
63. Laskowski, R. A.; MacArthur, M. W.; Moss, D. S.; Thornton, J. M. *J. Appl. Crystallogr.* **1993**, *26*, 283.
64. Bordi, F.; Mor, M.; Plazzi, P. V.; Silva, C.; Morini, G.; Caretta, A.; Barocelli, E.; Impicciatore, M. *Farmaco* **1992**, *47*, 1343.
65. Boeckler, F.; Lanig, H.; Gmeiner, P. *J. Med. Chem.* **2005**, *48*, 694.
66. Ligneau, X.; Garbarg, M.; Vizuete, M. L.; Diaz, J.; Purand, K.; Stark, W.; Schunack, W.; Schwartz, J.-C. *J. Pharmacol. Exp. Ther.* **1994**, *271*, 452.
67. Vacondio, F.; Mor, M.; Silva, C.; Zuliani, V.; Rivara, M.; Rivara, S.; Bordi, F.; Plazzi, P. V.; Magnanini, F.; Bertoni, S.; Ballabeni, V.; Barocelli, E.; Carrupt, P. A.; Testa, B. *Eur. J. Pharm. Sci.* **2004**, *23*, 89.
68. Berman, H. M.; Westbrook, J.; Feng, Z.; Gilliland, G.; Bhat, T. N.; Weissig, H.; Shindyalov, I. N.; Bourne, P. E. *Nucleic Acids Res.* **2000**, *28*, 235.
69. Paesen, G. C.; Adams, P. L.; Harlos, K.; Nuttall, P. A.; Stuart, D. I. *Mol. Cell* **1999**, *3*, 661.
70. Shi, L.; Javitch, J. A. *Annu. Rev. Pharmacol. Toxicol.* **2002**, *42*, 437.
71. Liu, C.; Ma, X.-J.; Jiang, X.; Wilson, S. J.; Hofstra, C. L.; Blevitt, J.; Pyati, J.; Li, X.; Chai, W.; Carruthers, N.; Lovenberg, T. W. *Mol. Pharmacol.* **2001**, *59*, 420.
72. Cheng, Y. C.; Prusoff, W. H. *Biochem. Pharmacol.* **1973**, *22*, 3099.
73. Furchgott, R. F. In Blanschko, E., Muscholl, E., Eds.; Handbook of Experimental Pharmacology; Springer: Berlin, 1972; Vol. 33, pp 283–335.
74. Higgins, D. G.; Sharp, P. M. *Gene* **1988**, *73*, 237 <www.ch.embnet.org/software/ClustalW.html>.
75. States, D. J.; Gish, W.; Altschul, S. F. *Methods: A Companion to Methods in Enzymology* **1991**, *3*, 66.
76. SYBYL 6.8., Tripos Inc., 1699 South Hanley Road, St. Louis, MO 63144, USA.
77. Halgren, T. A. *J. Comput. Chem.* **1996**, *17*, 490.
78. Fletcher, R.; Powell, M. *Comput. J.* **1963**, *6*, 63.
79. The Scripps Research Institute, La Jolla, CA, USA.
80. Morris, G. M.; Goodsell, D. S.; Halliday, R. S.; Huey, R.; Hart, W.; Belew, R. K.; Olson, A. J. *J. Comput. Chem.* **1998**, *19*, 1639.
81. Mohamadi, F.; Richards, N. G. J.; Guida, W. C.; Liskamp, R.; Lipton, M.; Caufield, C.; Chang, G.; Hendrickson, T.; Still, W. C. *J. Comput. Chem.* **1990**, *11*, 440.